Utility of AdaBoost to Detect Sleep Apnea-Hypopnea Syndrome From Single-Channel Airflow

Gonzalo C. Gutiérrez-Tobal*, *Student Member, IEEE*, Daniel Álvarez, *Member, IEEE*, Félix del Campo, and Roberto Hornero, *Senior Member, IEEE*

Abstract—Goal: The purpose of this study is to evaluate the usefulness of the boosting algorithm *AdaBoost* (AB) in the context of the sleep apnea-hypopnea syndrome (SAHS) diagnosis. *Methods:* We characterize SAHS in single-channel airflow (AF) signals from 317 subjects by the extraction of spectral and nonlinear features. Relevancy and redundancy analyses are conducted through the fast correlation-based filter to derive the optimum set of features among them. These are used to feed classifiers based on linear discriminant analysis (LDA) and classification and regression trees (CART). LDA and CART models are sequentially obtained through AB, which combines their performances to reach higher diagnostic ability than each of them separately. *Results:* Our AB-LDA and AB-CART approaches showed high diagnostic performance when determining SAHS and its severity. The assessment of different apnea-hypopnea index cutoffs using an independent test set derived into high accuracy: 86.5% (5 events/h), 86.5% (10 events/h), 81.0% (15 events/h), and 83.3% (30 events/h). These results widely outperformed those from logistic regression and a conventional event-detection algorithm applied to the same database. *Conclusion:* Our results suggest that AB applied to data from single-channel AF can be useful to determine SAHS and its severity. *Significance:* SAHS detection might be simplified through the only use of single-channel AF data.

*Index Terms—*AdaBoost (AB), airflow (AF), sleep apnea-hypopnea syndrome (SAHS), spectral analysis, nonlinear analysis.

I. INTRODUCTION

IN recent years, the sleep apnea-hypopnea syndrome (SAHS) has become a major concern due to the high prevalence and severe consequences for the patients' health and quality of life [1], [2]. People suffering from SAHS experiment recurrent episodes of complete (apnea) or partial (hypopnea) collapse of the upper airway during sleep, which lead to cessation or significant reduction of airflow (AF) [3]. These apneic events cause oxygen desaturations and arousals [3], preventing patients from resting while sleeping [2]. Unsuccessful rest derives in daytime symptoms such as hypersomnolence, cognitive impairment, and depression [1], some of which have been related to motor-vehicle collisions and occupational accidents [4], [5]. Moreover, SAHS has been associated with cardiac and vascular illnesses [2], as well as with an increase in the cancer incidence [6].

The standard test to diagnose SAHS is overnight in-lab polysomnography (PSG) [3]. Although its effectiveness is well known, PSG implies monitoring and recording multiple physiological signals, including electrocardiogram (ECG), electroencephalogram (EEG), electromyogram (EMG), oxygen saturation of blood (SpO$_2$), and AF [3]. This makes PSG a complex test which requires expensive equipment and technical expertise [7], [8]. Moreover, the specialists need an offline inspection of the recordings to derive the apnea-hypopnea index (AHI), which is the parameter used to establish SAHS and its severity [9]. Thus, PSG is also time consuming, leading to a delayed diagnostic process and increased waiting lists [8], [10].

One widespread approach to reduce complexity, cost, and time delay is the study of a limited set of signals among those involved in PSG [8]. The analysis of a single one has been often adopted. Thus, the oxygen desaturation index (ODI) from SpO$_2$, the apneic-related events from ECG, and the respiratory disturbance index (RDI) from AF have been already assessed to help in SAHS diagnosis [10]–[13]. These works followed a common methodology: detecting the effects caused by each apnea and hypopnea in the signals under study, scoring them as apneic-related events, and deriving the corresponding diagnostic index. However, our research group has lately adopted a different approach based on an exhaustive analysis of a signal through the extraction of global features [14]–[18].

In this paper, we propose such a global analysis in single-channel AF. AF is a straightforward choice to look for simpler alternatives to PSG, since apneas and hypopneas are defined on the basis of its amplitude oscillations [9]. The American Academy of Sleep Medicine (AASM) recommends the use of two AF channels: one acquired through an oronasal thermal sensor and the second one acquired by means of a nasal prong pressure sensor (NPP) [9]. The former is suitable for a proper scoring of apneas whereas the latter is used to score hypopneas [9]. However, previous studies have shown that it is possible to reach high diagnostic ability following an automatic global analysis of the single-channel AF from a thermal sensor [17], [18]. In this paper, one major goal is to assess whether it is also possible to reach a high performance when using data from single-channel AF obtained by NPP.

*G. C. Gutiérrez-Tobal is with the Biomedical Engineering Group, University of Valladolid, 47002 Valladolid, Spain (e-mail: gonzalo.gutierrez@gib.tel.uva.es).

D. Álvarez, and R. Hornero are with the Biomedical Engineering Group, University of Valladolid.

F. del Campo is with the Sleep Unit, Hospital Universitario Rio Hortega.

Our proposal starts with the extraction of spectral (frequency domain) and non-linear (time domain) features from NPP AF. The analysis in frequency domain is justified due to the overnight recurrence of these events. Thereby, common spectral features have already shown their utility to characterize SAHS as well as other disorders [15]–[19]. On the other hand, non-linear measures of variability, complexity, and irregularity in time series have been also used to extract useful information from biomedical signals [14], [17]–[19]. This exhaustive characterization of AF, however, may lead to obtain features with a high degree of shared information, i.e., redundant features. In order to avoid this issue, a second step is included in our methodology: an automatic feature selection stage based on the fast correlation-based filter (FCBF) [20]. The FCBF algorithm selects optimum sets of features on the basis of their relevancy and redundancy. It has been also assessed in biomedical applications [17], [21]. Finally, a classification approach is used to distinguish SAHS and its severity. Thus, we evaluate two different cases: a binary classification task, in which the objective is to determine the presence (SAHS-positive) or absence (SAHS-negative) of SAHS, and a multiclass task, in which the aim is to assess the AHI cutoffs which establish the four severity levels of SAHS (no-SAHS, mild-SAHS, moderate-SAHS, and severe-SAHS). We propose the *AdaBoost* (AB) algorithm for both classification tasks. AB is a boosting algorithm commonly used to take advantage of the performance of several weak classifiers of the same type [22]. It is known to be able to reach high yields when it is applied to new data [22], i.e., the AB algorithm produces generalized models. Moreover, it relies on a simple sequential procedure [22], which barely increases the complexity of the methodology. These characteristics make it a suitable algorithm to be used in diagnostic aid contexts. Actually, it has been already assessed in the context of SAHS under a classic event-detection approach [23], [24]. As weak classifiers we propose two well-known machine learning algorithms based on 1) linear discriminant analysis (LDA) and 2) classification and regression trees (CART). Both of them have been already assessed in the context of SAHS [16], [23]. Since classifiers favor the right sorting of classes with more subjects, one major issue in the present work is how to deal with imbalanced classes. The high prevalence of SAHS leads to prioritize diagnosis in at-risk population [25]. Consequently, data from SAHS patients is more available than from no SAHS subjects. Thus, to compensate for this imbalance, we use the synthetic minority oversampling technique (SMOTE) [26], which creates new synthetic data from the minority classes on the basis of the real data.

Our hypothesis is that the information obtained from AF and the generalization ability of AB can be useful to automatically detect SAHS and establish its severity. Thus, the main objective of the present work is to evaluate the diagnostic usefulness of AB when the only source of SAHS-related information is single-channel AF from NPP. In order to achieve this goal, we evaluate whether our proposal outperforms the diagnostic ability of a typical classification algorithms such as logistic regression (LR), which is based on one single classifier. We also apply to our AF recordings an algorithm focused on the classical event-detection approach, which has been previously assessed in other

TABLE I
DEMOGRAPHIC AND CLINICAL DATA FOR THE TWO-CLASS DIVISION

	All	SAHS-Negative	SAHS-Positive
# Subjects	317	110	207
Age (years)	49.9 ± 12.0	47.6 ± 12.9	51.1 ± 11.4
Men (%)	226 (71.3)	68 (61.8)	158 (76.3)
BMI (kg/m^2)	28.1 ± 5.2	26.5 ± 5.0	29.0 ± 5.1
AHI (e/h)	28.1 ± 26.5	6.0 ± 2.6	39.9 ± 25.9

TABLE II
DEMOGRAPHIC AND CLINICAL DATA FOR THE FOUR-CLASS DIVISION

	no-SAHS	Mild	Moderate	Severe
# Subjects	39	92	70	116
Age (years)	43.9 ± 12.5	50.3 ± 12.4	49.9 ± 11.3	51.6 ± 11.5
Men (%)	19 (48.7)	58 (63.0)	56 (80.0)	93 (80.2)
BMI(kg/m^2)	26.0 ± 5.5	27.0 ± 4.6	28.5 ± 3.9	29.5 ± 5.8
AHI (e/h)	3.0 ± 1.3	8.6 ± 2.4	22.2 ± 4.1	55.7 ± 24.7

databases [17], [27]. Finally, our results are also compared with other recent studies focused on SAHS detection from single-channel AF.

II. POPULATION AND SIGNAL UNDER STUDY

In this study, AF recordings from 317 adults were involved. Before undergoing PSG, all of the subjects suffered from common symptoms such as daytime sleepiness, loud snoring, nocturnal choking and awakenings, and/or referred apneic events. PSG was conducted in the sleep unit of the Hospital Universitario Río Hortega in Valladolid, Spain. Physicians scored apneas and hypopneas according to the AASM rules [9]. Consequently, an apnea was defined as a 90% or more reduction in the preevent baseline of the AF amplitude, measured through an oronasal thermal sensor. In contrast, a hypopnea was scored after 30% or more reduction in the preevent baseline of the AF amplitude, measured through a nasal pressure sensor, and accompanied by a drop of 3% in SpO$_2$ and/or an EEG arousal. In both cases, duration of 10 s or more was required to annotate the event [9]. All the subjects gave their informed consent and the Ethics Committee of the Hospital Universitario Rio Hortega (Spain) accepted the protocol.

Common AHI cutoffs to determine SAHS and its severity are 5, 10, 15, and 30 e/h [9], [10], [13], [17]. Particularly, SAHS severity levels are: no-SAHS ($5 < \text{AHI}$), mild-SAHS ($5 \leq \text{AHI} < 15$), moderate-SAHS ($15 \leq \text{AHI} < 30$), and severe-SAHS ($\text{AHI} > 30$) [28]. Alternatively, $\text{AHI} = 10$ e/h has been widely used as cutoff to determine the presence or absence of SAHS [10], [13], [17], [18], [29]. Consequently, for the binary classification task, we chose $\text{AHI} = 10$ e/h to distinguish SAHS-negative and SAHS-positive subjects, whereas for the multiclassification task, we divided our database according to the four SAHS severity levels. Tables I and II show clinical and demographical data of the subjects under study when they are divided for the binary or the multiclass tasks, respectively. No statistically significant differences were found (*p*-value > 0.01)

between SAHS-positive and SAHS-negative (Mann–Whitney U test), or among the four severity levels (Kruskal–Wallis test), in body mass index (BMI) and age.

The AF recordings were obtained during overnight PSG, which was performed through a polysomnograph (E-series, Compumedics). An NPP sensor was used to acquire AF (sample rate = 128 Hz). The recording length was 7.4 ± 0.3 h (mean ± standard deviation). An antialiasing filter was applied to the AF recordings to satisfy the Nyquist–Shannon theorem. We also applied an infinite impulse response Butterworth low-pass filter (cutoff = 1.2 Hz) to reduce noise for a prospective nonlinear analysis in time domain.

We divided our recordings into a training set (60%) and a test set (40%). A uniformly random selection was conducted to assign the AF recordings to each one. However, for the sake of the balance of the classes in the training set, we fixed the size of each class as follows: 29 no-SAHS subjects, 54 mild-SAHS, 54 moderate-SAHS, and 54 severe-SAHS. This distribution in the multiclass problem leads to 75 SAHS-negative and 116 SAHS-positive for the binary classification task. The SMOTE algorithm was used to compensate the remaining imbalance in classes of the training set (see section III-F). The recordings not selected for the training set were assigned to the test set.

III. METHODS

Our methodology consists of three steps. First, a feature extraction stage is implemented, in which spectral and nonlinear analyses are conducted over the AF recordings. Then, an automatic feature selection is performed to obtain an optimum set of the extracted features. Finally, a boosting classification approach is adopted to determine SAHS (binary classification) and its severity (multiclass task). Fig. 1 depicts a block diagram with the entire methodology followed during the study, which is widely explained in next sections.

A. Feature Extraction

1) Spectral Analysis: Apneas and hypopneas recurrently modify AF throughout the night. This behavior supports its study in the frequency domain. Hence, the power spectral density (PSD) of each AF recording was estimated. Welch's method was applied for this purpose since it is suitable for nonstationary signals [30]. A Hamming window of 2^{15} points (50% overlap), along with a discrete Fourier transform of 2^{16} points, were used to compute PSD. To avoid the influence of factors not related to the pathophysiology of SAHS, each PSD was normalized (PSDn) dividing the amplitude value at each frequency by their corresponding total power [31]. Fig. 2(a) shows the averaged PSDn for the four SAHS severity groups in the training set.

A spectral band of interest (BW) was defined between 0.025 Hz and 0.050 Hz [see Fig. 2(b)]. This corresponds to events lasting from 20 to 40 s, which has been reported as the typical range of the apneic events duration [32]. Moreover, BW is consistent with the bands found through statistical approaches [17], [18]. Thus, to characterize SAHS, nine spectral features were extracted from the 0.025–0.050 Hz band of each PSDn: minimum amplitude (*mA*), maximum amplitude (*MA*),

317 AF recordings from NPP

Feature extraction:
9 spectral features
3 non-linear features

12 extracted features

Feature selection: (training set only)
Fast Correlation-Based Filter (FCBF)

Optimum feature set

Ensemble learning classification:

AdaBoost training (LDA and CART)   (training set only)
(Bootstrap for model parameter setting)

Binary   Multiclass
(with SMOTE)   (with SMOTE)

Trained models   Trained models

Ensemble learning classification:
AdaBoost testing (LDA and CART)   (test set only)
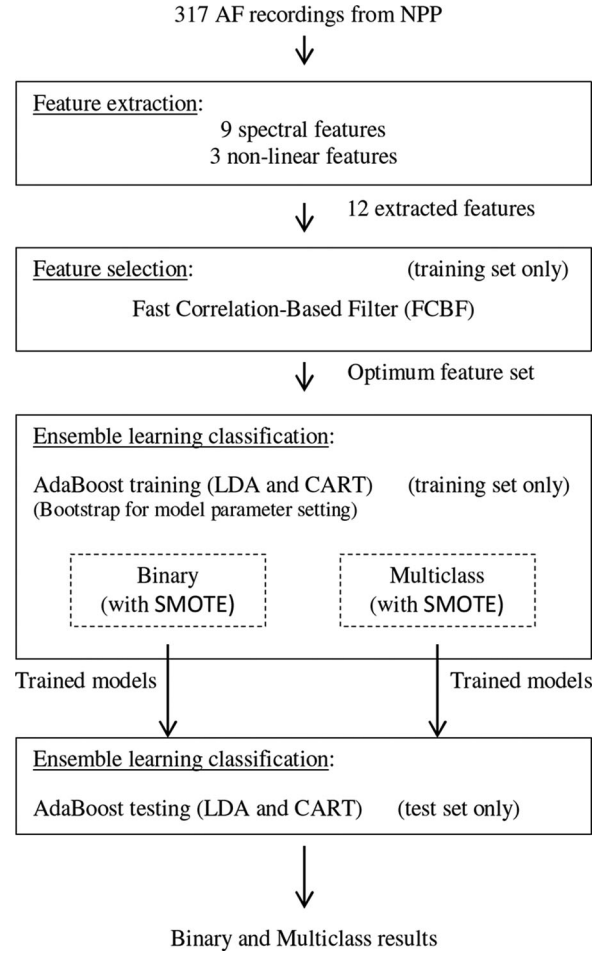
Binary and Multiclass results

Fig. 1.   Block diagram of the signal processing methodology followed during the study.

first to fourth statistical moments ($M_{f1} - M_{f4}$), median frequency (*MF*), spectral entropy (*SpecEn*), and Wootters distance (*WD*).

mA and *MA* were computed as the lowest and the highest PSDn values in BW. Since PSD is normalized, the amplitude values of the original AF time series do not affect the power at each frequency component. Hence, as BW is related to apneic events, *mA* and *MA* estimate the minimum and the maximum occurrence of them. Mean (M_{f1}), standard deviation (M_{f2}), skewness (M_{f3}), and kurtosis (M_{f4}) of BW were also obtained. They are common statistics that quantify central tendency, dispersion, asymmetry, and peakedness of data, respectively. According to Fig. 2(b), *mA* and *MA* should be higher as SAHS worsens. Similarly, the mean (M_{f1}) and the standard deviation (M_{f2}) should be also higher. Finally, both the skewness (M_{f3}) and the peakedness (M_{f4}) seem to be higher in the BW spectral data of moderate and severe groups.

MF is defined as the frequency component that separates the spectrum into two parts with 50% of the power each of them [33]. Thus, the lower the *MF* value, the more comprised is the spectrum into small frequencies. As seen in Fig 2(b), the spectrum of BW for the no-SAHS and mild-SAHS groups is flat, i.e., the power is equally distributed. Conversely, a fewer
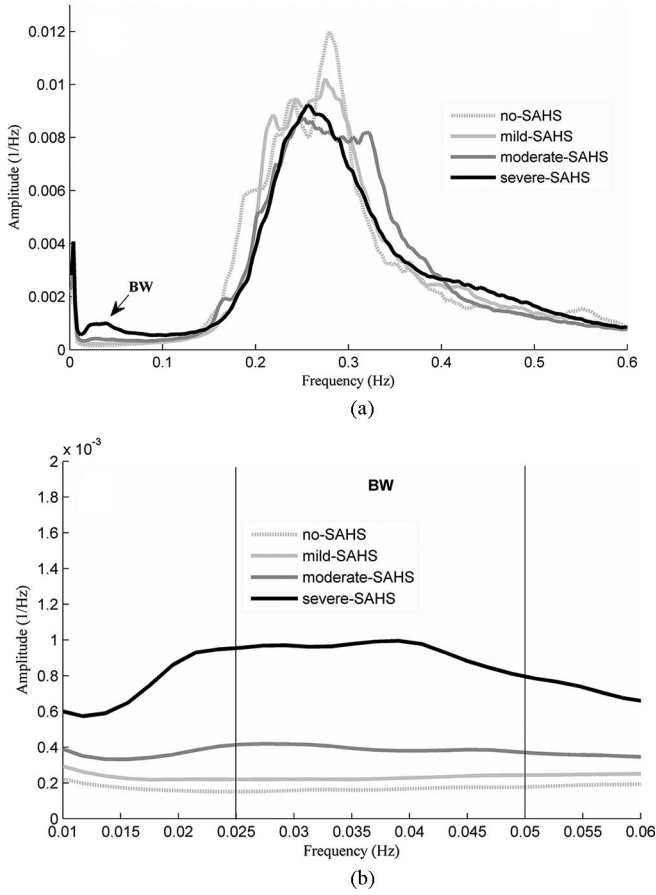
Fig. 2. (a) Averaged PSDn for the four SAHS severity groups in the training set and b) detail of the band of interest BW.

amount of power is observed in higher frequencies of BW for moderate-SAHS and severe-SAHS groups. As a consequence, an *MF* value closer to 0.0375 (the half of the band) is expected for the lowest severity degrees.

SpecEn quantifies the flatness of the PSD content, which indirectly measures the irregularity of time series [33]. Thereby, high values of *SpecEn* are related to a flat PSD (similar to white noise), and consequently, it is associated with more irregularity in time domain. By contrast, low values imply a spectrum condensed into a narrow frequency band, which is related to less irregularity in time domain (like in a sum of sinusoids) [33]. A flatter spectrum is observed in BW as SAHS severity decreases. Therefore, higher values of *SpecEn* are expected in no-SAHS and mild-SAHS groups.

WD is a disequilibrium measure that assigns values close to 1 to those distributions with higher statistical distance to the uniform distribution; whereas values close to zero are assigned as the distance becomes smaller [34], [35]. In BW, the averaged spectrum of the no-SAHS and mild-SAHS groups is similar to a normal distribution [see Fig. 2(b)]. Hence, smaller values of *WD* are expected than in the case of the moderate-SAHS and severe-SAHS groups.

2) Nonlinear Analysis: Alterations caused by SAHS in AF could modify the variability, the complexity, and the irregularity of the signal. Hence, to complement the spectral analysis,

three global nonlinear features were also obtained from each recording in time domain: central tendency measure (*CTM*), Lempel–Ziv complexity (*LZC*), and sample entropy (*SampEn*). Similarly to PSD, each AF time series was normalized before obtaining *CTM*, *LZC*, and *SampEn*. Thereby, measuring effects caused by factors not related to the pathophysiology of SAHS are avoided. We first eliminated the spurious values of the signal. Then, the time series were divided by the remaining maximum absolute value in order to constrain each recording into the range −1, 1.

CTM quantifies the variability of a given series $x[n]$ on the basis of its first-order differences [36]. These are plotted following $x[n+2] - x[n+1]$ vs. $x[n+1] - x[n]$ [37]. The value of *CTM* is computed as the proportion of points in the plot, which fall within a radius ρ [36], which acts as a design parameter. Thus, *CTM* ranges between 0 and 1, with higher values corresponding to points more concentrated around the center of the plot, i.e., corresponding to less degree of variability. People suffering from SAHS experiment continuous changes in the respiratory pattern (apneic events, snoring, choking, respiratory overexertion after apneas and hypopneas), which may add variability to the AF signal. Consequently, it is expected that *CTM* decreases in the presence of SAHS.

LZC estimates the complexity of a finite sequence of symbols [38]. Hence, the first step of the algorithm is to convert a time series $x[n]$ into such a sequence [37]. Usually, a binary transformation is performed, with the median of each $x[n]$ being used as threshold [37]. Then, the sequence is scanned, and a counter $c(n)$ is increased with every new subsequence of consecutive symbols. Finally, $c(n)$ is normalized in order to make the method independent of the sequence length. The higher the value of *LZC*, the higher the complexity of the corresponding time series is [37]. Abnormalities in the AF pattern may introduce new subsequences of symbols. Hence, more complexity is expected in the AF of SAHS patients.

SampEn is a measure of the irregularity in time series [39]. It was developed by Richman and Moorman to reduce the bias caused by self-matching in the estimation of the approximate entropy [40]. *SampEn* divides a time series into consecutive vectors of length m. It assesses whether the maximum absolute distance between the corresponding components of each pair of vectors is less than or equal to a tolerance r, i.e., if the vectors match each other within r. If so, the vectors are considered as similar. Then, the same process is repeated for vectors of length $m+1$ and the conditional probability that similar vectors of length m remain similar when the length is $m+1$ is computed. The final *SampEn* value is obtained as the negative logarithm of such a conditional probability [39], [40]. Thus, higher values of *SampEn* indicate less self-similarity in the times series, and consequently, more irregularity [39]. SAHS is reflected in the AF signal by the addition of not regular events. As a consequence, it is expected that *SampEn* present higher values in SAHS patients.

B. Feature Selection: Fast Correlation-Based Filter

The exhaustive characterization of the AF signal may lead to the extraction of several features that provide similar

information about SAHS, i.e., which are redundant. Hence, a feature selection stage is included to discard those features (X_i), which share more information with the others than with a SAHS-related-dependent variable, Y. The FCBF has shown its utility in previous studies involving SAHS [17], as well as other biomedical applications [21]. In our case, Y is a vector whose components are the AHI value of each subject.

FCBF relies on symmetric uncertainty (SU), which is a normalized quantification of the information gain (IG) between two variables [20]. It consists of two steps. In the first one, a relevance analysis of the features (X_i) is done. Thus, SU between each feature X_i and Y is computed as follows:

$$SU(X_i, Y) = 2 \left[\frac{IG(X_i|Y)}{H(X_i) + H(Y)} \right] \quad i = 1, 2, ..., F \quad (1)$$

where $IG(X_i|Y) = H(X_i) - H(X_i|Y)$, H is the well-known Shannon's entropy, and F is the number of features extracted ($F = 12$). SU is constrained to 0–1. A 0 value indicates that the two variables are independent, whereas $SU = 1$ indicates that knowing one feature it is possible to completely predict the other [20]. Thus, the higher the value of SU, the more information shares the corresponding feature with the AHI, and consequently, the more relevant is. Then, a ranking of features is done based on their $SU(X_i, Y)$ values, i.e., from most relevant to least relevant. The second step is a redundancy analysis in which the SU between each pair of features ($SU(X_i, X_j)$) is sequentially estimated beginning from the first-ranked ones. If $SU(X_i, X_j) \geq SU(X_i, Y)$, with X_i being more highly ranked than X_j, the feature j is discarded due to redundancy and is not considered in next comparisons [20]. The optimum features are those not discarded when the algorithm ends.

C. Classification Approach: Boosting

After the feature selection procedure, each subject from our database is associated with a vector $\mathbf{x}_k$ ($k = 1, 2, \ldots, N$, where N is the size of our sample), whose components are the values of the features included in the optimum set. The purpose is to build models with the ability to determine SAHS and its severity on the basis of the information contained in the vectors $\mathbf{x}_k$. Boosting procedures are known to achieve good generalization ability [22]. Thus, 60% of the instances are used as training set ($N_{\mathrm{training}} = 191$) to feed the boosting method AB, which we use along with LDA and CART as weak classifiers (AB-LDA and AB-CART). The remaining 40% ($N_{\mathrm{test}} = 126$) is used as test group to validate the models. For comparison purposes, we also train a classic logistic regression (LR) classifier.

1) AB Algorithm: Boosting procedures are iterative algorithms designed to combine models that complement one another [22]. Such a combination is conducted on the basis of weighted votes from classifiers of the same type [22], [41]. AB is a widely used boosting algorithm, originally developed by Freund and Schapire [42], which can be used along with any classifier [22]. However, if AB is applied to complex classifiers, the prediction ability on new data may be significantly decreased [22], i.e., its generalization ability may be lost. Thus, simpler

procedures known as weak classifiers are preferable [22]. In our case, we chose the well-known LDA and CART algorithms to act as weak classifiers.

At each m iteration, the AB algorithm assigns a weight, w_k^m, to every instance (or vector) $\mathbf{x}_k$ in the training set. Thus, the mth weak classifier is trained using the corresponding weighted instances. Then, its performance is assessed through an error ε_m. This error is used to determine the weighted vote, α_m, of this mth classifier [22]. Thereby, those classifiers with smaller ε_m contribute more to the final decision. At the end of the iteration, the weights of the misclassified instances are updated (w_k^{m+1}) [22]. Then, the weights of all instances are normalized in order to maintain the original distribution [42].

Two versions of AB have been implemented in this study: AB.M1, for binary classification, and AB.M2 for the multiclass task. Both of them rely on reweighting those instances, which have been misclassified after each iteration. Thus, the weak classifier trained during the next iteration gives more importance to these instances [42], being more likely to classify them rightly [22]. The main difference between AB.M1 and AB.M2 is how the error ε is defined. For AB.M1, ε_m is the sum of the weights of the misclassified instances in a given iteration m, divided by the sum of the total weights of all instances at that iteration.

$$\varepsilon_m = \frac{\sum_{k=1}^{N_{\mathrm{training}}} w_k^m \,(\mathrm{miss.})}{\sum_{k=1}^{N_{\mathrm{training}}} w_k^m}. \quad (2)$$

By contrast, a weighted pseudoloss is defined in the case of AB.M2, for which ε_m is as follows [42]:

$$\varepsilon_m = \frac{1}{2} \cdot \sum_{k=1}^{N_{\mathrm{training}}} \sum_{c \neq c_{\mathrm{true}}} w_{k,c}^m \cdot (1 - h_m(\mathbf{x}_k, c_{\mathrm{true}}) + h_m(\mathbf{x}_k, c)) \quad (3)$$

where c is a categorical variable representing the multiple classes, c_{true} refers to the actual class of $\mathbf{x}_k$, and h_m is the confidence of the prediction of the weak learner for an instance $\mathbf{x}_k$ and a class from c.

AB.M1 and AB.M2 perform the final classification task by returning the class with the highest sum of the votes from all classifiers, taking into account the weight of their corresponding predictions α_m computed as follows [42]:

$$\alpha_m = \ln(\beta_m) \quad (4)$$

where β_m is defined as $(1 - \varepsilon_m)/\varepsilon_m$. Additionally, the shrinkage regularization technique has been proposed to minimize overfitting [43]. It is based on adding a learning rate υ to the iterative process by redefining β_m as $(\beta_m)^\upsilon$, where υ ranges 0−1 and has to be experimentally estimated.

Two criteria were used to stop the AB.M1 algorithm: 1) ε_m does not belong to the interval (0, 0.5) [22] or 2) the number of weak learners is not higher than 400 (to minimize the overfitting chances). In the case of AB.M2, only the second criterion was applied since the first one is considered too restrictive for multiclass approaches [42].

D. Logistic Regression and Conventional Approach Algorithm

We also implemented LR models and a conventional event-detection algorithm to evaluate them using our own database.

LR is a widely used supervised learning algorithm, which has become a standard for binary classification tasks [44]. It estimates the posterior probability that a given instance (or vector) $\mathbf{x}_k$ belongs to one of two classes. First, the LR algorithm uses the maximum likelihood estimation of the coefficients of a linear transformation where the dependent variables are the components of each $\mathbf{x}_k$ [44], in our case, features extracted from the signals. Then, the well-known logit function is applied to this linear transformation in order to obtain the aforementioned probability [44]. Vector $\mathbf{x}_k$ is then assigned to the class with the highest posterior probability.

We also implemented a conventional scoring algorithm in order to apply it to our AF recordings database. Thus, a peak detection algorithm was used to locate inspiratory onsets and endings in AF time series [45]. The difference between AF values in consecutive onsets and endings locations determined the amplitude of every inspiration. According to the rules of the AASM, the algorithm scored those respiratory events, which meet with 1) a drop of 30% or more from the AF preevent baseline and 2) the drop lasts 10 s or more [9]. The baseline was computed as the mean amplitude of the s previous inspirations [27]. Hence, s was a design parameter. Once all events are scored, the total amount of them is divided by the sleep time to obtain an AHI estimation. To choose an optimum s value, we computed the AHI estimations of the subjects in the training group, with s ranging 1–10. For each s, the Spearman's correlation was computed between the corresponding AHI estimations and the actual AHI from the subjects. The highest correlation was obtained for $s = 6$, which was established as the optimum value.

E. Statistical Analysis

The extracted features did not pass the Lilliefors normality test. Hence, the nonparametric Kruskal–Wallis test was used to establish significant statistical differences between the four groups of SAHS severity (p-value < 0.01). Bonferroni correction was applied to deal with multiple comparisons. Diagnostic ability of the AB and LR models was assessed in terms of sensitivity (Se, percentage of positive subjects rightly classified), specificity (Sp, percentage of negative subjects rightly classified), accuracy (Acc, overall percentage of subjects rightly classified), and Cohen's kappa (κ). κ measures the agreement between predicted and observed classes, avoiding the part of agreement by chance [22].

The bootstrap 0.632 algorithm [22], which was only applied to the training group, was used to find an optimum learning rate υ for the AB models. Thus, B new bootstrap training groups (B_{training}), with the same size as the original one, were built by resampling with replacement from this [46]. We chose $B = 500$ since it suffices for a proper estimation of the error, while let the variance remain low [46]. A uniform probability was used to select from the original instances in the training group. Consequently, some of these instances were repeated for each

new B_{training}, whereas the same number remained unemployed. The latter were used as the corresponding bootstrap test groups (B_{test}). We evaluated υ in the range (0, 1] (step = 0.1). At each step, we computed κ^n ($n = 1, 2, \ldots, B$) as follows [22]:

$$\kappa^n = 0.369 \cdot \kappa^n_{B\,\mathrm{training}} + 0.632 \cdot \kappa^n_{B\,\mathrm{test}} \tag{5}$$

where $\kappa^n_{B\,\mathrm{training}}$ and $\kappa^n_{B\,\mathrm{test}}$ are the Cohen's kappa values for each B_{training} and B_{test}, respectively. Then, the 500 κ^n statistics were averaged in each step, and υ was chosen according to the highest κ averaged value.

F. Balancing the Classes: SMOTE

Before training the classifiers, we applied SMOTE to compensate the imbalance among classes. SMOTE creates new synthetic instances on the basis of the available minority class real ones [26]. In our case, the real instances are the vectors of features associated to each subject in this minority class. According to the number of new instances (vectors) required for the compensation of the classes, the algorithm selects the K-nearest neighbors of each of the real ones [26]. Thus, if it is required to double the minority class vectors, K should be 1, and so on. Then, the difference between each vector and its K-nearest neighbors is computed. These differences, multiplied by a random number in the range 0 to 1, are subsequently, added to the original vector again, to form new synthetic ones whose components are between the vector considered and its corresponding K-nearest neighbors [26].

As it can be derived from Table II, our instances of features, $\mathbf{x}_k$, come from: 39 no-SAHS, 92 mild-SAHS, 70 moderate-SAHS, and 116 severe-SAHS. These were divided into a training (60%) and a test set (40%). Since the training set plays the key role to avoid the bias toward majority classes [26], we adjusted its configuration to balance the classes as much as possible. Hence, although the inclusion of instances into the training set was uniformly random per class, we forced to include 29 no-SAHS, 54 mild-SAHS, 54 moderate-SAHS, and 54 severe SAHS. Then, we applied SMOTE ($K = 1$) to the instances of the no-SAHS class to create 29 additional synthetic ones. Consequently, the balanced training set was finally composed of 58 no-SAHS, 54 mild-SAHS, 54 moderate-SAHS, and 54 severe SAHS. Accordingly, the test set was composed of 10 no-SAHS, 38 mild-SAHS, 16 moderate-SAHS, and 62 severe-SAHS.

This instance distribution, carried out for the four classes, also resulted in a balanced training set for the binary classification task. Thus, it was composed of 104 SAHS-negative instances (75 real and 29 synthetic) and 116 SAHS-positive instances (all real). The test set was composed of 35 SAHS-negative instances and 91 SAHS-positive instances.

IV. RESULTS

A. Feature Extraction and Selection

The optimum values for ρ (*CTM*), as well as m and r (*SampEn*), were obtained by evaluating the ranges $\rho \in [0.001, 0.1]$ (step $= 0.001$), and $m = 1, 2$ and $r \in [0.10^*\mathrm{SD}, 0.25^*\mathrm{SD}]$ (step $= 0.05^*\mathrm{SD}$), where SD is the standard deviation of the time

TABLE III
FEATURE VALUES FOR THE SEVERITY GROUPS (MEAN ± SD)

Feat.	no-SAHS	Mild	Moderate	Severe	p-value
MA (10^{-4})	2.012 ± 1.091	2.854 ± 1.460	5.148 ± 3.134	13.736 ± 11.360	$\ll 0.01$
mA (10^{-4})	1.359 ± 0.729	1.849 ± 0.930	2.903 ± 1.294	6.225 ± 4.498	$\ll 0.01$
M_{f1} (10^{-4})	1.670 ± 0.912	2.296 ± 1.131	3.900 ± 1.886	9.400 ± 7.295	$\ll 0.01$
M_{f2} (10^{-5})	2.140 ± 1.424	3.193 ± 2.428	7.418 ± 8.268	24.864 ± 27.774	$\ll 0.01$
M_{f3}	0.190 ± 0.540	0.259 ± 0.512	0.149 ± 0.619	0.429 ± 0.689	0.19^{+}
M_{f4}	2.154 ± 0.590	2.269 ± 0.569	2.298 ± 0.637	2.608 ± 1.115	0.41^{+}
WD	0.046 ± 0.019	0.052 ± 0.029	0.063 ± 0.041	0.086 ± 0.056	0.003^{+}
MF	0.038 ± 0.001	0.038 ± 0.002	0.037 ± 0.002	0.036 ± 0.002	0.004^{+}
$SpecEn$ (10^{-1})	9.963 ± 0.032	9.958 ± 0.046	9.924 ± 0.168	9.882 ± 0.134	0.024^{+}
CTM (10^{-1})	9.993 ± 0.007	9.988 ± 0.015	9.987 ± 0.009	9.963 ± 0.023	$\ll 0.01$
LZC	0.057 ± 0.009	0.057 ± 0.007	0.057 ± 0.006	0.058 ± 0.007	0.71^{+}
$SampEn$	0.059 ± 0.012	0.063 ± 0.014	0.062 ± 0.016	0.058 ± 0.014	0.18^{+}

$^{+}$ *Not lower than Bonferroni correction (p-value = 0.01/6).*

series. In the case of ρ, the range was chosen according to the character of data [36]. Thus, values of $\rho < 0.001$ were discarded since they led to a *CTM* value ≈ 0 regardless the SAHS severity group of the subjects. Similarly, values of $\rho > 0.1$ were also not considered since they led to *CTM* values $= 1$ for every subject. The ranges of m and r were suggested by Pincus (2001) as those that experimentally produced a good entropy estimation in time series longer than 60 samples [47]. We chose those configurations ($\rho = 0.05$ for *CTM* and $m = 2$ and $r = 0.1*$SD for *SampEn*) for which the corresponding *CTM* and *SampEn* values showed the highest Spearman's correlation with the variable composed of the AHI measures from the subjects. We only used training data for this purpose. Table III shows the values of the extracted features for the SAHS severity levels in the training set (mean $\pm$ SD only from the real instances), along with the corresponding p-values. Four out of the nine spectral features (*MA*, *mA*, M_{f1}, and M_{f2}), as well as *CTM*, showed statistical significant differences among classes after the Bonferroni correction (p-value < 0.01). These spectral features showed higher values as the SAHS severity increased. An opposite tendency was shown by *CTM* values. Thus, the variability also increased with the severity of SAHS.

The FCBF was also applied to the training set (only real instances). According to FCBF, the ranking of the 12 extracted features, from higher to lower *SU* values, was: M_{f1}, *MA*, *CTM*, *mA*, M_{f2}, *WD*, *SpecEn*, *MF*, M_{f4}, *LZC*, M_{f3}, and *SampEn*. Then, *WD* was found redundant with M_{f2}; and M_{f3} with *MF*. Hence, the final FCBF optimum set was composed of ten features, seven from BW (M_{f1}, *MA*, *mA*, M_{f2}, *SpecEn*, *MF*, and M_{f4}) and three from the nonlinear analysis (*CTM*, *LZC*, and *SampEn*).

B. Classification

1) Model Selection and Training: The AB binary models (AB-LDA$_2$ and AB-CART$_2$) were selected according to the optimum υ value. Fig. 3 displays the corresponding averaged κ values for each υ after the bootstrap 0.632 algorithm. As mentioned earlier, this procedure was only applied to the training set. The maximum values of κ for AB-LDA$_2$ and AB-CART$_2$ (0.602 and 0.713, respectively) were reached at $\upsilon = 0.1$ and $\upsilon = 0.6$.
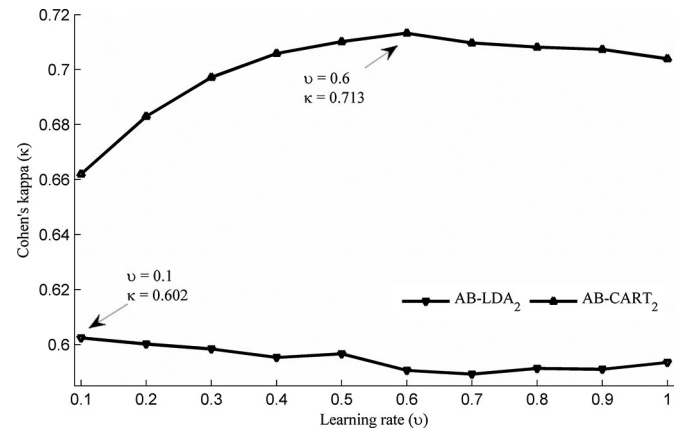

Fig. 3. Optimum υ configuration for AB-LDA$_2$ and AB-CART$_2$ (obtained after bootstrap process).

Then, the whole original training set was used along with these υ values to train the AB-LDA$_2$ and AB-CART$_2$ models. AB-LDA$_2$ ended after 53 iterations ($\varepsilon_{54} \geq 0.5$). Hence, 53 LDA models were taken into account for the final classification task. AB-CART$_2$ reached the limit of learners established. Therefore, it was assessed in the bootstraps sets with more weak learners (500–1000). No improvement in κ was reached. Consequently, the weighted votes of 400 CART models were used for the classification.

For the case of the AB multiclass models (AB-LDA$_4$ and AB-CART$_4$), we optimized both the learning rate and the number of learners (up to 400) during the bootstrap procedure. Hence, for each value of υ between 0 and 1 (step $= 0.1$) we varied the number of weak learners from 1 to 400 (step $= 10$) in order to compute κ. Fig. 4 displays the values of κ as a function of υ and the number of weak learners. For AB-LDA$_4$, the optimum values were $\upsilon = 1$ along with 110 weak learners, whereas for AB-CART$_4$, were $\upsilon = 0.8$ and 160 weak learners.

2) Performance of the Models: Table IV shows the diagnostic ability of the binary models (test set). The highest values for Acc and κ are shown in bold. AB-CART$_2$ outperformed the other models in Se, Acc, and κ, as well as reached the highest Sp along with LR. These results show its higher diagnostic
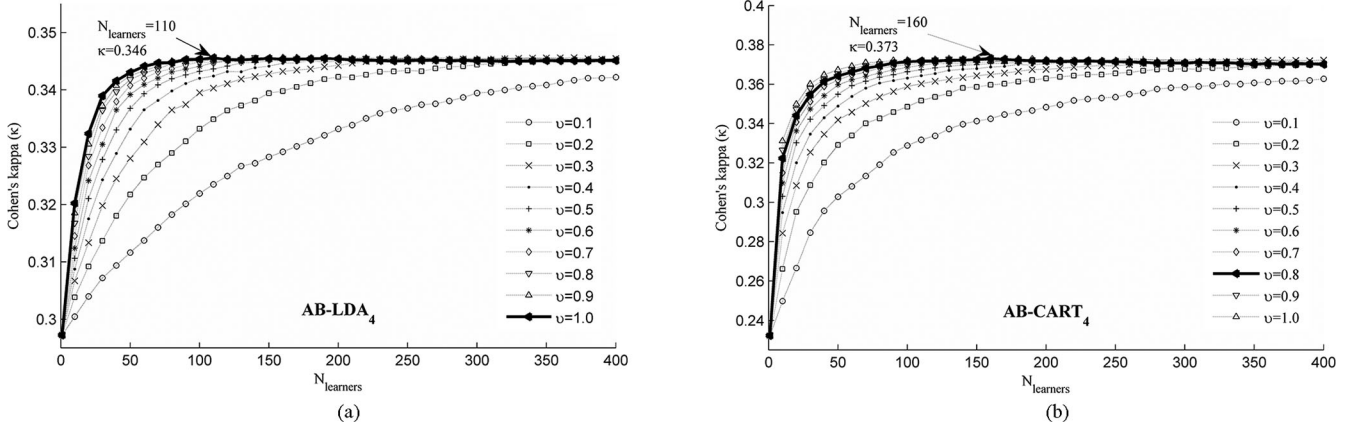
Fig. 4. Optimum υ and number of weak learners for a) AB-LDA$_4$ and b) AB-CART$_4$ (obtained after the bootstrap process).

TABLE IV
DIAGNOSTIC ABILITY OF THE BINARY MODELS IN THE TEST SET

Models	Se (%)	Sp (%)	Acc (%)	κ
Event-detec.	75.8	54.3	69.0	0.286
LR	83.5	80.0	82.5	0.593
LDA$_2$	72.5	74.3	73.0	0.410
CART$_2$	85.7	68.6	81.0	0.593
AB-LDA$_2$	86.8	77.1	84.1	0.618
AB-CART$_2$	89.0	80.0	86.5	0.672

performance. AB-LDA$_2$ also improved the results from the classic event-detection algorithm and LR. However, the latter was more specific. Additionally, AB-LDA$_2$ and AB-CART$_2$ widely improved the performance of single models based on LDA and CART (LDA$_2$ and CART$_2$).

The lowest performance was reached by the algorithm based on the event-detection approach.

In the multiclass task, Table V displays the confusion matrices of each model, i.e., the model class estimation for each subject versus their actual SAHS severity group. Notice that, since it is a binary classifier, LR was evaluated following the one versus all strategy [41]. The overall accuracy (main diagonal) of the models and the event-detection algorithm was low in test set: event-detection 39.7%, LR 57.4%, AB-LDA$_4$ 60.3% (47.6% in the case of a single LDA$_4$ model), and AB-CART$_4$ 57.4% (54.8% in the case of a single CART$_4$ model). Classification of mild and moderate subjects was particularly poor for all the models. In contrast to the overall accuracy, the diagnostic performance increases when assessing the predictions of the models in each of the AHI severity cutoffs (5 e/h, 15 e/h, and 30 e/h). Table VI displays such performance for the multiclass models and the event-detection algorithm. Consistent with the overall accuracy, κ values are low. However, high diagnostic accuracies are reached by AB-LDA$_4$ and AB-CART$_4$. They outperformed LR and the event-detection algorithm in terms of Acc and κ when assessing the three AHI cutoffs. Finally, AB-LDA$_4$ widely improved the overall performance of single LDA$_4$, as well as the Acc for each AHI cutoff. AB-CART$_4$ also improved the overall performance of CART$_4$, as well as the Acc

for 5 e/h and 30 e/h. However, CART$_4$ outperformed the Acc of AB-CART$_4$ when considering 15 e/h as the AHI cutoff.

V. DISCUSSION AND CONCLUSION

In this paper, new methodologies to help in SAHS diagnosis have been proposed. Binary and multiclass AB models, composed of LDA and CART classifiers, have been evaluated to distinguish SAHS and its severity. Their performances were compared with a conventional approach (event-detection algorithm) and the classic LR classifier, both of them applied to our own database. AB outperformed these, showing high diagnostic ability.

Spectral and nonlinear data, extracted from single-channel AF from NPP, were the only source of SAHS-related information used to feed the models. The spectral analysis showed significantly higher spectral power (M_{f1}) and power spectral density (*MA* and *mA*) in the 0.025–0.050 Hz. frequency band as SAHS severity increased. Since we normalized the PSD values, these measures are related to a higher occurrence of the apneic events, and not with their amplitude. This supports these features as SAHS severity dependents. Dispersion (M_{f2}) in the PSDn values at BW was also significantly higher as SAHS worsened, suggesting a more heterogeneous occurrence of apneic events throughout the frequencies within BW. Finally, the nonlinear analysis showed significantly higher variability (lower *CTM* values) when SAHS severity increased. This is consistent with our initial assumption that the more severe SAHS the more changes in the respiratory pattern, and consequently, the higher variability in AF. These five features were selected by FCBF. Although M_{f2}, *SpecEn*, *MF*, *LZC*, and *SampEn* did not show discriminative power to distinguish SAHS severity, they were also automatically chosen, suggesting their usefulness by providing complementary information. Moreover, spectral and nonlinear features were included in the ten-feature FCBF optimum set, which indicates that one analysis complement the other, as suggested in previous studies involving AF from the thermistor [17], [18].

AB-CART$_2$ achieved the highest Acc and κ values for the binary (AHI cutoff = 10 e/h) classification task (86.5% Acc, 0.672

TABLE V
CONFUSION MATRICES FOR EACH MODEL IN THE TEST SET

		Event-Detection				LR (one vs. all)				AB-LDA$_4$ (LDA$_4$)				AB-CART$_4$ (CART$_4$)			
Estimated →		no	mild	mod.	severe	no	mild	mod.	severe	no	mild	mod.	severe	no	mild	mod.	severe
Actual	no-SAHS	2	4	3	1	8	0	2	0	8 (8)	0 (0)	2 (2)	0 (0)	8 (7)	1 (2)	1 (1)	0 (0)
	mild	12	16	5	5	14	8	10	6	11 (13)	16 (7)	8 (13)	3 (5)	14 (16)	8 (11)	12 (9)	4 (2)
	moderate	1	5	5	5	3	3	4	6	3 (5)	4 (2)	6 (6)	3 (3)	3 (4)	2 (3)	6 (6)	5 (3)
	severe	3	17	15	27	2	1	7	52	1 (4)	3 (5)	12 (14)	46 (39)	0 (3)	3 (0)	9 (14)	50 (45)

Results from LDA and CART single models in parentheses.

TABLE VI
DIAGNOSTIC ABILITY OF THE MULTICLASS MODELS IN THE TEST SET

	Event-Detection			LR (one vs. all)			AB-LDA$_4$ (LDA$_4$)			AB-CART$_4$ (CART$_4$)		
	5	15	30	5	15	30	5	15	30	5	15	30
Se (%)	86.2	66.7	43.5	83.6	88.5	83.9	87.1 (81.0)	85.9 (79.5)	74.2 (62.9)	85.3 (82.8)	89.7 (87.2)	80.6 (72.6)
Sp (%)	20.0	70.8	82.8	80.0	62.5	81.3	80.0 (80.0)	72.9 (58.3)	90.6 (87.5)	80.0 (70.0)	64.6 (75.0)	85.9 (92.2)
Acc (%)	81.0	68.3	63.5	83.3	78.6	82.5	**86.5** (81.0)	81.0 (71.4)	82.5 (75.4)	84.9 (81.7)	80.2 (**82.5**)	**83.3** (82.5)
κ		0.152			0.370			**0.432** (0.281)			0.381 (0.369)	

Results from LDA and CART single models in parentheses.

κ). In the multiclass classification, AB-LDA$_4$ obtained 86.5%, 81.0%, 82.5% Acc for 5 e/h, 15 e/h, and 30 e/h, respectively, as well as $\kappa = 0.432$. It is worth noting that both AB-LDA$_4$ and AB-CART$_4$ reached high statistics when evaluating 5 and 30 e/h. They outperformed the LR models, the single-model LDA and CART classifiers, as well as the event-detection algorithm. These cutoffs are particularly important. AHI = 5 e/h draws the line for the lower degree of SAHS. Furthermore, AHI = 30 e/h, which establish the boundary for the highest SAHS severity, has been associated with mortality [48], as well as suffices to recommend a treatment even in the absence of other symptoms [49]. In this regard, and according to Table V, 46 out of the 52 subjects (88.5%) that the AB-LDA$_4$ ensemble predicted as severe-SAHS were rightly classified, whereas the remaining 6 (11.5%) were mild- or moderate-SAHS, at least. Similarly, 50 out of the 59 subjects (84.7%) that the AB-CART$_4$ ensemble predicted as severe were indeed severe, with 0 subjects from the no-SAHS group falling within this class.

Table VII summarizes performances from previous works focused on the use of single-channel AF from NPP to help in SAHS diagnosis [10], [13], [50]–[52]. All studies, except the present one, adopted an event detection approach. When assessing AHI = 10 e/h, only Wong *et al.* achieved higher diagnostic performance than AB-CART$_2$ [10], [51]. However, a small sample size was used to evaluate their proposals. Nakano *et al.* detected apneic events in AF with the help of spectral analysis [50]. They reported higher Se (97.0%) but lower Sp (76.0%). Unfortunately, some data about the population under study, required to complete the comparison, were not reported by the authors. None of the studies, outperformed our AB-LDA$_4$ model (86.5% Acc) in the assessment of AHI = 5 e/h. However, Nakano *et al.* reported significantly higher Se (97.0%) [50]. Additionally, BaHammam *et al.* and Nigro *et al.* exhibited higher diagnostic ability when assessing AHI = 30 e/h [13], [52].

TABLE VII
COMPARISON WITH THE STATE OF THE ART OF SINGLE-CHANNEL AF FROM NPP

Studies	Subjects (n)	AHI Cutoff	Se (%)	Sp (%)	Acc (%)
[a]De Almeida *et al.* [10]	30	10	85.7	87.5	nd
[a]Nakano *et al.* [50]	217	5	97.0	77.0	nd
		10	97.0	76.0	nd
		15	97.0	73.0	nd
[a]Wong *et al.* [51]	33	10	92.0	86.0	90.9*
		30	91.0	75.0	81.5*
[a]BaHammam *et al.* [52]	95	5	79.0	68.0	76.8*
		10	70.0	89.0	77.9*
		15	65.0	94.0	81.8*
		30	63.0	98.0	83.2*
[a]Nigro *et al.* [13]	90	5	89.3	60.0	84.4*
		10	80.4	82.3	nd
		15	76.7	83.0	80.0*
		30	88.5	95.3	93.3*
[b]AB-CART$_2$	317	10	89.0	80.0	86.5
		5	87.1	80.0	86.5
[b]AB-LDA$_4$	317	15	85.9	72.9	81.0
		30	74.2	90.6	82.5

[a]*Event detection approach;* [b]*direct subject classification approach;* *computed from reported data; nd: not enough data to estimate.*

Nonetheless, their databases were composed of 95 and 90 subjects, respectively, in contrast to the 317 subjects involved in our study. Finally, all the studies performed similarly to our AB-LDA$_4$ model (81.0% Acc) when evaluating AHI = 15 e/h.

Despite we have shown the utility of our proposal, some limitations need to be addressed. Although our sample is large (317 subjects), analyzing more recordings would enhance the statistical power of our results. Particularly, a more balanced proportion of the classes would be desirable for the sake of the model training. Nonetheless, our sample reflects a realistic proportion among the people who undergo the PSG test. Additionally,

we applied the SMOTE technique to our data in order to compensate the imbalance. The single use of NPP to acquire AF may be another limitation. The AASM recommends using both NPP and thermistor for a proper quantification of the number of apneas and hypopneas [9]. However, our proposal does not rely on a classic event-detection approach. In this regard, previous studies of our research group showed high diagnostic ability when evaluating data from single-channel AF acquired through a thermistor [17], [18]. Our current proposal has shown that using AF data from NPP is also possible in order to reach a high diagnostic performance. Another limitation arises regarding the redundant information removed by the FCBF algorithm. The features discarded share more information with the selected ones than with the AHI. However, the features selected might still share information with the others to some extent. The training time of the AB models is another limitation if we compare it with simpler methodologies such as logistic regression. However, once the models are trained, the runtime after they are applied to new data is trivial. Finally, since we propose an automatic procedure with potential to reach diagnosis in few minutes after data collection, it would be of great interest if future works could address the assessment of our methodology embedded in a diagnostic test at patient's home. It would be also interesting the implementation and assessment of a multiclass logistic-regression-based AB algorithm.

To the best of our knowledge, this is the first time that the AB algorithm is used along with spectral and nonlinear features from single-channel AF to help in SAHS diagnosis. Our AB proposals for binary and multiclass classification outperformed the classic LR as well as a conventional event-detection algorithm, both of them applied to our own database. The new AB-CART$_2$ and AB-LDA$_4$ models achieved high diagnostic ability compared with the state of the art. Additionally, we showed that it is possible to achieve high diagnostic ability by the use of spectral and nonlinear data from NPP AF. These results highlight the usefulness of our proposal when detecting SAHS and its severity.

REFERENCES

[1] T. Young *et al.*, "Epidemiology of obstructive sleep apnea: A population health perspective," *Amer. J. Respir. Crit. Care. Med.*, vol. 165, pp. 1217–1239, 2002.

[2] F. Lopez-Jiménez *et al.*, "Obstructive sleep apnea," *Chest*, vol. 133, pp 793–804, 2008.

[3] S. P. Patil *et al.*, "Adult obstructive apnea," *Chest*, vol. 132, pp. 325–337, 2007.

[4] A. Sassani *et al.*, "Reducing motor-vehicle colissions, costs, and fatalities by treating obstructive sleep apnea syndrome," *Sleep*, vol. 27, pp. 453–458, 2003.

[5] E. Lindberg *et al.*, "Role of snoring and daytime sleepiness in occupational accidents," *Amer. J. Respir. Crit. Care Med.*, vol. 164, pp. 2031–2035, 2001.

[6] F. Campos-Rodriguez *et al.*, "Association between obstructive sleep apnea and cancer incidence in a large multicenter spanish cohort," *Amer. J. Respir. Crit. Care Med.*, vol. 187, pp. 99–105, 2013.

[7] J. A. Bennet and W. J. M. K. WJM, "Sleep on the cheap: the role of overnight oximetry in the diagnosis of sleep apnoea hypopnoea syndrome," *Thorax*, vol. 54, pp. 958–959, 1999.

[8] W. W. Flemons *et al.*, "Home diagnosis of sleep apnea: A systematic review of the literature," *Chest*, vol. 124, pp. 1543–1579, 2003.

[9] R. B. Berry *et al.*, "Rules for scoring respiratory events in sleep: update of the 2007 AASM manual for the scoring of sleep and associated events," *J. Clin. Sleep Med.*, vol. 8, no. 5, pp. 597–619, 2012.

[10] F. R. de Almeida *et al.*, "Nasal pressure recordings to detect obstructive sleep apnea," *Sleep Breath*, vol. 10, pp. 62–69, 2006.

[11] U. J. Magalang *et al.*, "Prediction of the apnea-hypopnea index from overnight pulse oximetry," *Chest*, vol. 124, pp. 1694–1701, 2003.

[12] T. Penzel *et al.*, "Systematic comparison of different algorithms for apnoea detection based on electrocardiogram recordings," *Med. Biol. Eng. Comput.*, vol. 40, pp. 402–407, 2002.

[13] C. A. Nigro *et al.*, "Comparison of the automatic analysis versus the manual scoring from ApneaLink^{TM} device for the diagnosis of obstructive sleep apnoea syndrome," *Sleep Breath*, vol. 15, pp. 679–686, 2011.

[14] C. Gómez *et al.*, "Complexity analysis of the magnetoencephalogram background activity in Alzheimer's disease patients," *Med. Eng. Phys.*, vol. 28, pp. 851–59, 2006.

[15] D. Álvarez *et al.*, "Multivariate analysis of blood oxygen saturation recordings in obstructive sleep apnea diagnosis," *IEEE Trans. Biomed. Eng.*, vol. 57, no. 12, pp. 2816–2824, Dec. 2010.

[16] J. V. Marcos *et al.*, "Automated detection of obstructive sleep apnea syndrome from oxygen saturation recordings using linear discriminant analysis," *Med. Eng. Phys.*, vol. 59, pp. 141–49, 2010.

[17] G. C. Gutiérrez-Tobal *et al.*, "Pattern recognition in airflow recordings to assist in the sleep apnoea–hypopnoea syndrome diagnosis," *Med. Biol. Eng. Comput.*, vol. 51, pp. 1367–80, 2013.

[18] G. C. Gutiérrez-Tobal *et al.*, "Linear and nonlinear analysis of airflow recordings to help in sleep apnoea-hypopnoea syndrome diagnosis," *Physiol. Meas.*, vol. 33, pp. 1261–75, 2012.

[19] R. Hornero *et al.*, "Spectral and nonlinear analyses of MEG background activity in patients with Alzheimer's disease," *IEEE Trans. Biomed. Eng.*, vol. 55, no. 6, pp. 1658–1665, Jun. 2008.

[20] L. Yu and H. Liu, "Efficient feature selection via analysis of relevance and redundancy," *J. Mach. Learn. Res.*, vol. 5, pp. 1205–1224, 2004.

[21] A. Aarabi *et al.*, "Automated neonatal seizure detection: A multistage classification system through feature selection based on relevancy and redundancy analysis," *Clin. Neurophysiol.*, vol. 117, pp. 328–340, 2006.

[22] I. H. Witten, E. Frank, and M. A. Hall, *Data Mining: Practical Machine Learning Tools and Techniques*. Burlington, MA, USA: Morgan Kaufmann, 2011.

[23] C. Morgenstern *et al.*, "Assessment of changes in upper airway obstruction by automatic identification of inspiratory flow limitation during sleep," *IEEE Trans. Biomed. Eng.*, vol. 56, no. 8, pp. 2006–2015, Aug. 2009.

[24] B. Xie and H. Minn, "Real-time sleep apnea detection by classifier combination," *IEEE Trans. Inf. Technol. Biomed. Eng.*, vol. 16, no. 3, pp. 469–477, May 2012.

[25] W. W. Flemons *et al.*, "Access to diagnosis and treatment of patients with suspected sleep apnea," *Amer. J. Respir. Crit. Care. Med.*, vol. 169, pp. 668–72, 2004.

[26] N. V. Chawla *et al.*, "SMOTE: Synthetic minority over-sampling technique," *J. Artif. Intell. Res.*, vol. 16, no. 1, pp. 321–357, 2002.

[27] J. Han *et al.*, "Detection of apnoeic events from single channel nasal airflow using 2nd derivative method," *Comput. Meth. Prog. Bio.*, vol. 98, pp. 199–207, 2008.

[28] A. Qureshi *et al.*, "Obstructive sleep apnea," *J. Allergy Clin. Immunol.*, vol. 112, pp. 643–651, 2003.

[29] A. S. Karunajeewa *et al.*, "Multi-feature snore sound analysis in obstructive sleep apnea–hypopnea syndrome," *Physiol. Meas.*, vol. 32, no. 1, pp. 83–97, 2011.

[30] P. D. Welch, "The use of fast fourier transform for the estimation of power spectra: A method based on time averaging over short, modified periodograms," *IEEE Trans. Audio Electroacoust.*, vol. AU-15, no. 2, pp. 70–73, Jun. 1967.

[31] L. Sörnmo and P. Laguna, *Bioelectrical Signal Processing in Cardiac and Neurological Applications*, New York, NY, USA: Academic, 2005.

[32] D. J. Eckert and A. Malhotra, "Pathophysiology of adult obstructive sleep apnea," in *Proc. Amer. Thorac. Soc.*, 2008, vol. 5, pp. 144–153.

[33] J. Poza *et al.*, "Extraction of spectral based measures from MEG background oscillations in Alzheimer's disease," *Med. Eng. Phys.*, vol. 29, pp. 1073–1083, 2007.

[34] W. K. Wootters, "Statistical distance and Hilbert space," *Phys. Rev. D*, vol. 23, no. 2, pp. 357–362, 1981.

[35] M. T. Martin *et al.*, "Statistical complexity and disequilibrium," *Phys. Lett. A*, vol. 311, no. 2, pp. 126–132, 2003.

[36] M. E. Cohen *et al.*, "Applying continuous chaotic modeling to cardiac signal analysis," *IEEE Eng. Med. Biol. Mag.*, vol. 15, no. 5, pp. 97–102, Sep./Oct. 1996.

[37] D. Abásolo *et al.*, "Analysis of EEG background activity in Alzheimer's disease patients with Lempel–Ziv complexity and central tendency measure," *Med. Eng. Phys.*, vol. 28, no. 4, pp. 315–322, 2006.

[38] J. Ziv and A. Lempel, "Compression of individual sequences via variable-rate coding," *IEEE Trans. Inf. Theory*, vol. 24, no. 5, pp. 530–536, Sep. 1978.

[39] D. Abásolo *et al.*, "Entropy analysis of the EEG background activity in Alzheimer's disease patients," *Phys. Meas.*, vol. 27, pp. 241–253, 2006.

[40] J. S. Richman and J. R. Moorman, "Physiological time-series analysis using approximate entropy and sample entropy," *Amer. J. Physiol Heart Circ. Physiol.*, vol. 278, pp. H2039–H2049, 2000.

[41] C. M. Bishop, *Pattern Recognition and Machine Learning*, New York, NY, USA: Springer, 2006.

[42] Y. Freund and R. E. Schapire, "A decision-theoretic generalization of on-line learning and an application to boosting," *J. Comput. System Sci.*, vol. 55, no. 1, pp. 119–139, 1997.

[43] J. H. Friedman, "Greedy function approximation: A gradient boosting machine," *Ann. Statist.*, vol. 29, pp. 1189–1232, 2001.

[44] D. W. Hosmer and S. Lemeshow, *Applied Logistic Regression*. New York, NY, USA: Wiley, 2000.

[45] J. B. Korten and G. G. Haddad, "Respiratory waveform pattern recognition using digital techniques," *Comput. Biol. Med.*, vol. 19, pp. 207–217, 1989.

[46] B. Efron and R. J. Tibshirani, *An Introduction Bootstrap*. Boca Raton, FL, USA: CRC press, 1994.

[47] S. M. Pincus, "Assessing serial irregularity and its implications for health," *Ann. NY. Acad. Sci.*, vol. 954, pp. 245−267, 2001.

[48] N. M. Punjabi *et al.*, "Sleep-disordered breathing and mortality: A prospective cohort study," *PLoS med.*, vol. 6, no. 8, e1000132, 2009.

[49] P. Lloberes *et al.*, "Diagnosis and treatment of sleep apnea-hypopnea syndrome," *Arch. Bronconeumol.*, vol. 47, no. 3, pp. 143–156, 2011.

[50] H. Nakano *et al.*, "Automatic Detection of Sleep-disordered breathing from a single-channel airflow record," *Eur. Respir. J.*, vol. 29, pp. 728–736, 2007.

[51] K. K. Wong *et al.*, "Diagnostic test evaluation of a nasal flow monitor for obstructive sleep apnea detection in sleep apnea research," *Behavior Res. Methods*, vol. 40, no. 1, pp. 360–366, 2008.

[52] A. BaHammam *et al.*, "Evaluation of the accuracy of manual and automatic scoring of a single airflow channel in patients with a high probability of obstructive sleep apnea," *Med. Sci. Monit.*, vol. 17, pp. MT13–MT19, 2011.

Authors' photographs and biographies are not available at the time of publication.